Mechanical Erosion Modeling of TPS Materials

Sergio Fraile Izquierdo[1], Jeremie B.E. Meurisse[1], Georgios Bellas Chatzigeorgis[1], Nagi N. Mansour[1]

[1]Analytical Mechanics Associates Inc. at NASA Ames Research Center, Moffett Field, CA 94035, USA

12th Ablation Workshop
Lexington, KY - November 9-10, 2022

Mechanical erosion in TPS materials

For ablative thermal protection materials, the term mechanical erosion, also known as spallation, refers to the physical removal of solid particles from the ablating surface. This may result in an increased total surface recession and must be taken into account for heatshield modeling during atmospheric entry. This phenomenon has been extensively studied in the literature over the last decades by numerous authors [1–3], and the following mechanisms have been identified as the main causes: external forces on the heatshield's surface like shear stress and pressure from the flow field, thermal stress induced by the material's temperature field, normal stress induced by pyrolysis gas build-up, and shrinkage due to pyrolysis of the material. How much each of these mechanisms and factors contribute to the spallation process is not clear. This poster describes a modeling framework based on The Porous material Analysis Toolbox (PATO) [4] to account for mass removal due to mechanical erosion of TPS materials.

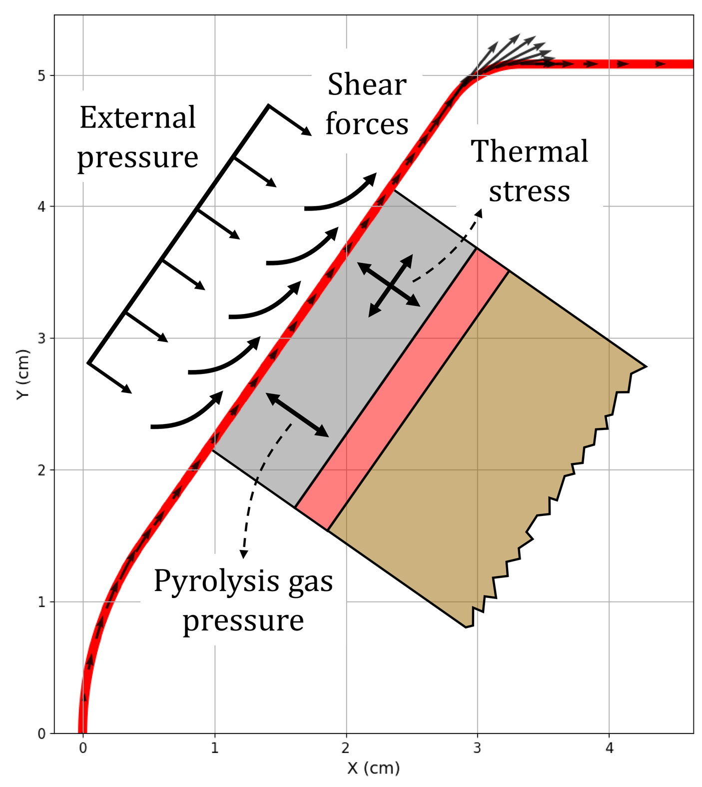

Fig. 1 Spallation mechanisms.

Implementation of the model in PATO

Assuming small strains and small rotations, the conservation of linear momentum solved in PATO follows [5, 6]:

$$\frac{\partial}{\partial t}\int_{\Omega_0} \rho \frac{\partial u}{\partial t}\, d\Omega_0 = \underbrace{\oint_{\Gamma_0} n_0 \cdot (K \cdot \nabla u)\, d\Gamma_0}_{\text{Implicit Term}} + \underbrace{\oint_{\Gamma_0} n_0 \cdot \sigma\, d\Gamma_0 - \oint_{\Gamma_0} n_0 \cdot (K \cdot \nabla u)\, d\Gamma_0}_{\text{Explicit Terms}} + \int_{\Omega_0} \rho\, b\, d\Omega_0$$

Where $K \cdot \nabla u$ is an approximation of the stress field in terms of the displacement field. This segregated solution approach allows us to solve the governing equation independently for each direction, while the coupling is achieved with outer iterations. Both, isotropic and orthotropic constitutive laws are implemented, and the solver also accounts for the thermal stress.

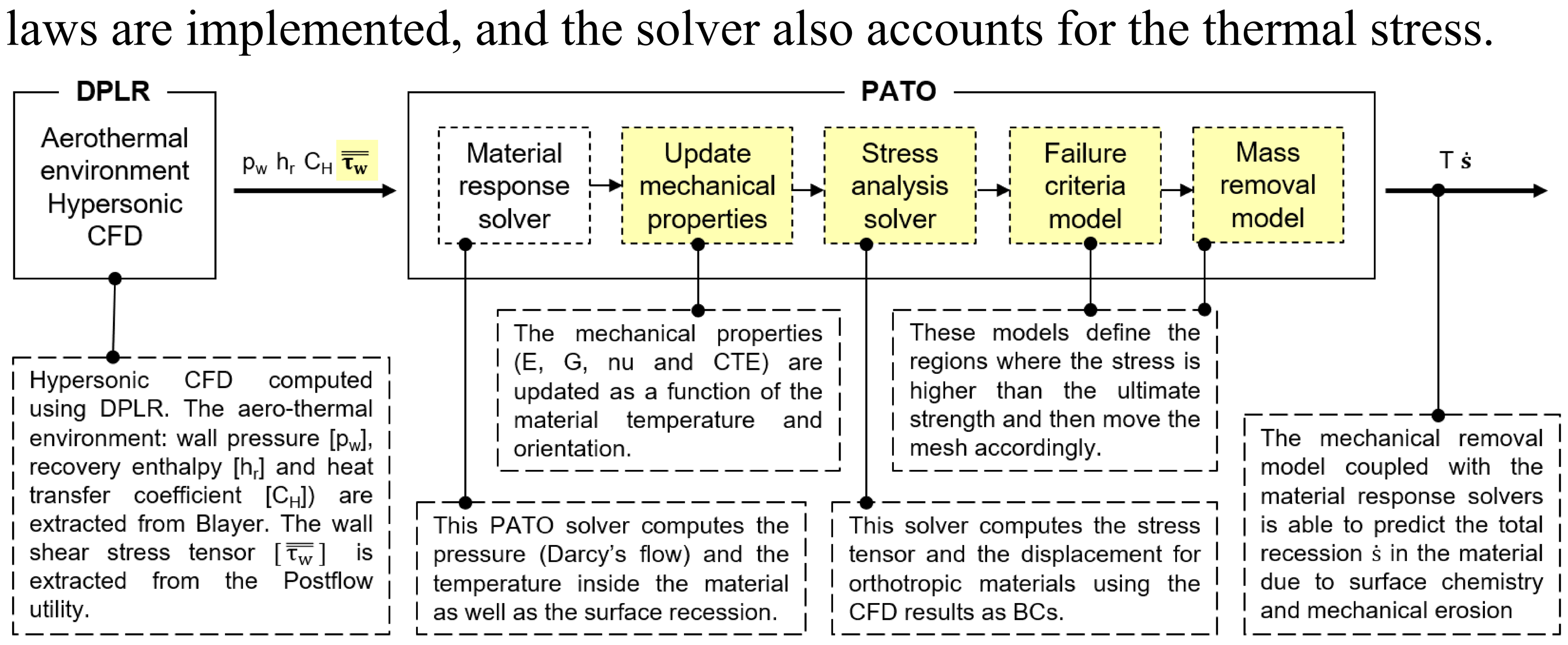

Fig. 5 Flow diagram of the mechanical erosion model implemented in PATO.

Stress analysis solver validation

The orthotropic stress analysis solver was verified against the open-source FEA package Code-Aster. Excellent agreement is found between the results despite the use of different formulations (finite volume vs finite element) and the limited grid refinement. Additional validation cases were also carried out to verify the implementation of the thermal stress component.

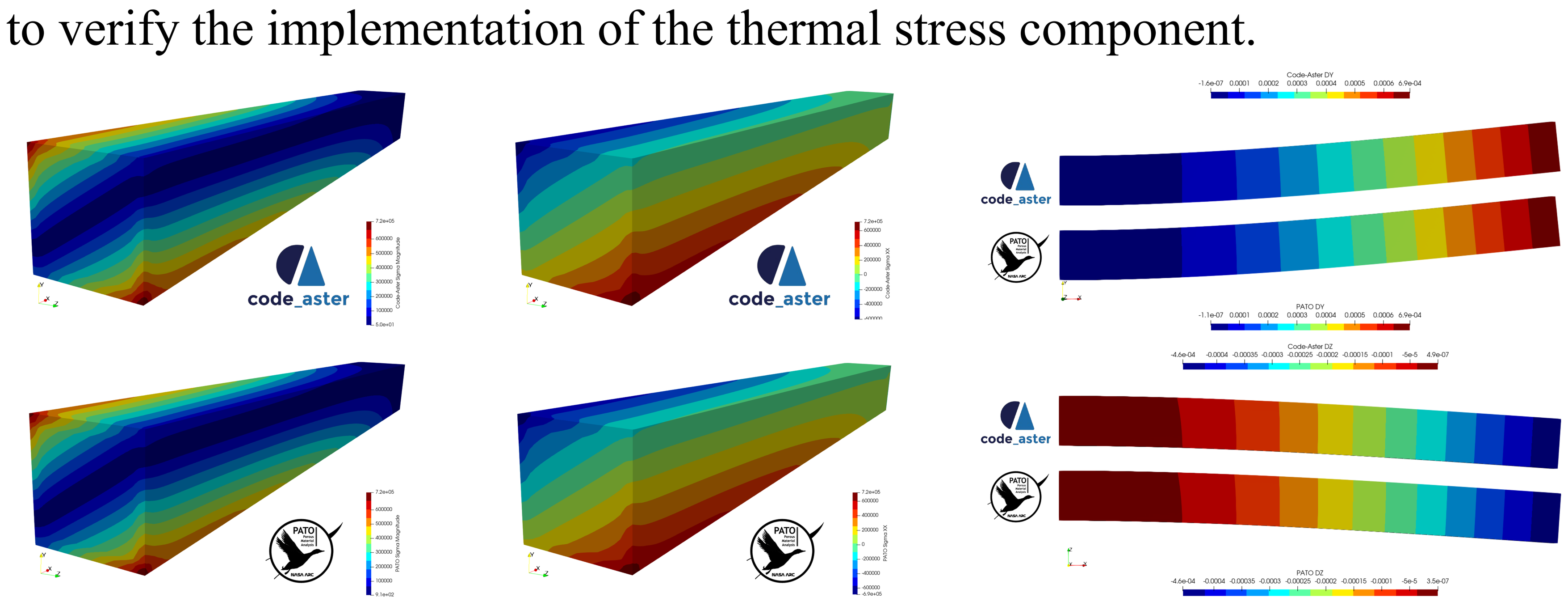

Fig. 6 Comparison results from PATO and Code-Aster: sigma magnitude (left), sigma XX (center), Y displacement (top-right), and Z displacement (bottom-right).

Computation of the material orientation

Depending on the manufacturing process of the TPS material, the orthotropic local orientation of each cell may not match the global coordinate system. As a result, it is necessary to compute the material orientations in order to assign the right mechanical properties to orthotropic materials. To this end, a PATO utility was developed to compute the rotation tensors used for stress analysis.

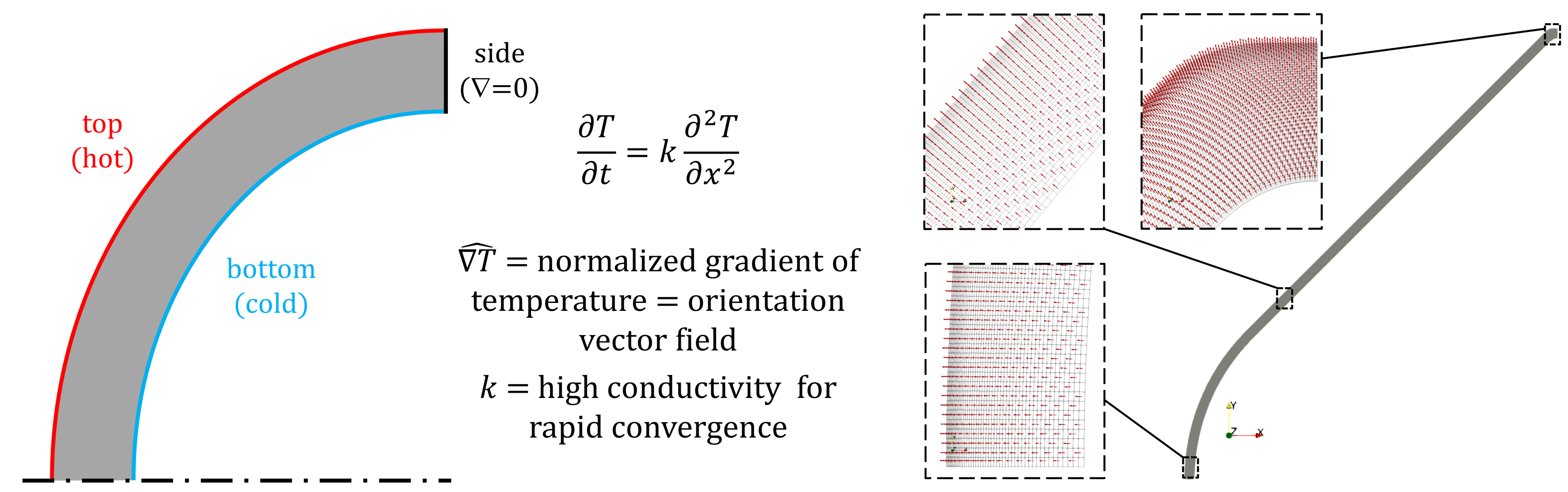

Fig. 6 Schematic diagram used to compute the material orientation (left), and material orientation of a typical heatshield geometry computed with PATO (right).

Mechanical properties as function of temperature

Mechanical properties are affected by the material's operating temperature. Usually, the material's stiffness and strength remain relatively stable around room temperature and gradually start to fall off as temperature increases [7]. This phenomena is of great importance for TPS materials due to the extreme temperatures they have to withstand. The simulations below model the mechanical behavior of an arc-jet test sample including shear stress, thermal expansion, mechanical properties as function of temperature, and ablation.

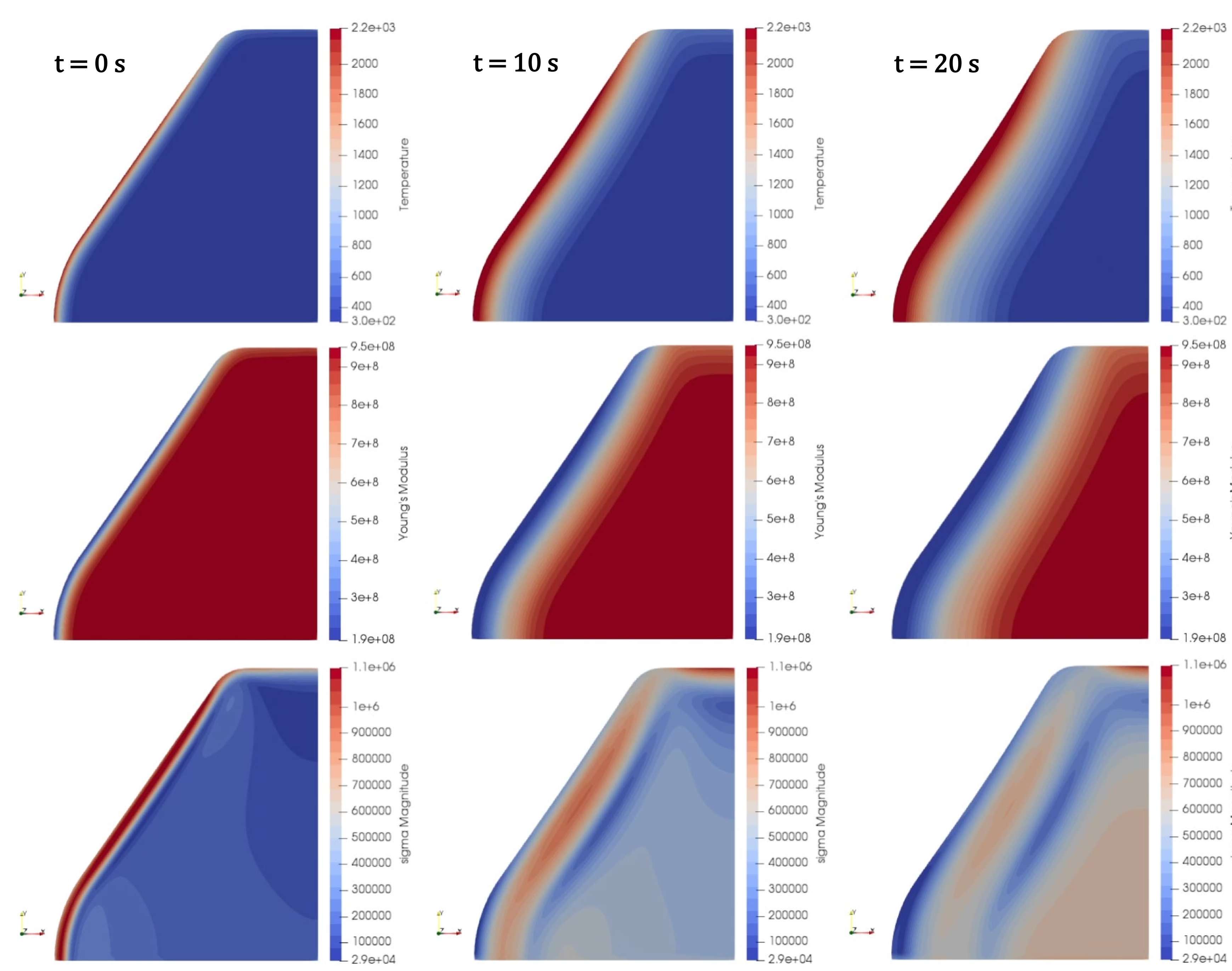

Fig. 7 Temperature, pressure, Young's modulus and sigma fields for temperature dependent mechanical properties (shear + thermal expansion) coupled with ablation.

Failure criteria and mass removal model

The failure criteria follows the maximum stress failure theory [8], where the maximum stresses of each mode (normal and shear) are compared to the ultimate strength. When a region connected to the surface fails, it is removed using the dynamic mesh motion solver. This allows for the computation of the mass loss, M_{loss}, and recession rate, $\dot{s}$, due to mechanical erosion.

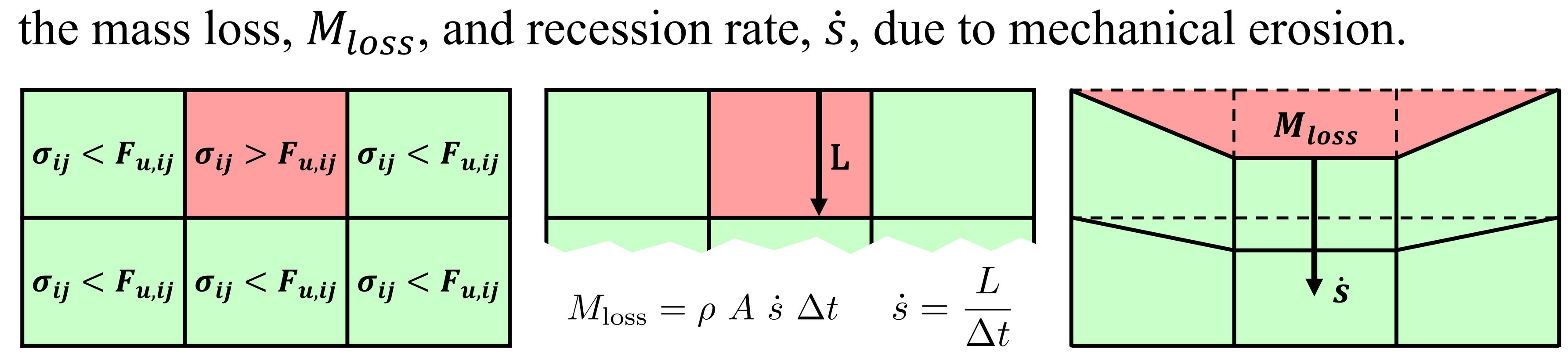

Fig. 9 Failure criteria (left), failing distance (L) using mesh search algorithm with $\dot{s}$ and M_{loss} equations (center), and mass removal using dynamic mesh motion (right).

References

[1] P. J. Schneider *et al.* (1968), *AIAA Journal.*
[2] J. Sullivan *et al.* (1987), *22nd Thermophysics Conference.*
[3] F. Grigat *et al.* (2020), *AIAA Scitech 2020.*
[4] J. Meurisse *et al.* (2018), *Aerospace Science and Technology*.
[5] P. Cardiff *et al.* (2014), *Comp. Methods in Appl. Mechanics and Eng.*
[6] I. Demirdžić *et al.* (2000), *Comp. Methods in Appl. Mechanics and Eng.*
[7] R. Tellers *et al.* (2008), Orbital *ATK Launch Systems.*
[8] A. A. Baker *et al.* (2004), *AIAA Publication.*